Proc. Natl. Acad. Sci. USA
Vol. 96, pp. 1941–1946, March 1999
Biochemistry

Mg-chelatase of tobacco: The role of the subunit CHL D in the chelation step of protoporphyrin IX

SUSANNA GRÄFE*, HANS-PETER SALUZ*, BERNHARD GRIMM†, AND FRANK HÄNEL*‡

*Hans-Knöll-Institut für Naturstoff-Forschung e.V., Department of Cell and Molecular Biology, Beutenbergstr. 11, 07745 Jena, Germany; and †Institut für Pflanzengenetik und Kulturpflanzenforschung, AG Chlorophyll Biosynthesis, Corrensstr. 3, 06466 Gatersleben, Germany

Edited by Lawrence Bogorad, Harvard University, Cambridge, MA, and approved December 21, 1998 (received for review July 20, 1998)

ABSTRACT **The Mg-chelation is found to be a prerequisite to direct protoporphyrin IX into the chlorophyll (Chl)-synthesizing branch of the tetrapyrrol pathway. The ATP-dependent insertion of magnesium into protoporphyrin IX is catalyzed by the enzyme Mg-chelatase, which consists of three protein subunits (CHL D, CHL I, and CHL H). We have chosen the Mg-chelatase from tobacco to obtain more information about the mode of molecular action of this complex enzyme by elucidating the interactions *in vitro* and *in vivo* between the central subunit CHL D and subunits CHL I and CHL H. We dissected CHL D in defined peptide fragments and assayed for the essential part of CHL D for protein–protein interaction and enzyme activity. Surprisingly, only a small part of CHL D, i.e., 110 aa, was required for interaction with the partner subunits and maintenance of the enzyme activity. In addition, it could be demonstrated that CHL D is capable of forming homodimers. Moreover, it interacted with both CHL I and CHL H. Our data led to the outline of a two-step model based on the cooperation of the subunits for the chelation process.**

Chelatases catalyze the insertion of divalent metal ions into tetrapyrroles. The multiple tetrapyrrole endproducts contain various metal cations, such as Mg(II), Fe(II), Co(II), Ni(II), Zn(II), Mn(II), and Cu(II), which are inserted by chelatases. The detailed mechanism of these enzymes is still not clear. Best known are the Mg and Fe chelatases (1). The Mg-chelatase is found to be specific for photosynthetic organisms. It catalyzes the insertion of the magnesium ion into protoporphyrin IX, the last common intermediate precursor in chlorophyll (Chl) and heme biosynthesis. The enzyme Fe chelatase plays an essential role in heme synthesis by catalyzing the insertion of a ferrous ion into the tetrapyrrole ring structure. Both of these enzymes use the same substrate, protoporphyrin IX (1). Despite this fact, the structure of these two proteins is entirely different. While the Mg-chelatase consists of three protein subunits, the ferrochelatase consists of only one protein (2).

In bacteriochlorophyll (Bch)-synthesizing *Rhodobacter sphaeroides* and *Chlorobium vibrioforme* as well as in the chlorophyll a-synthesizing cyanobacterium *Synechocystis*, the ORFs *bchD*/*chlD*, *bchH*/*chlH*, and *bchI*/*chlI* encode the proteins that are required for the reconstruction of *in vitro* Mg-chelatase activity (3–5). The proteins Bch H and Bch I of *R. sphaeroides* were purified to homogeneity, and the protein Bch D was partially purified (6). It was shown that a monomer of H and a dimer of I gave optimal Mg-chelatase activity (6). Furthermore, *Xantha-f*, *-g,* and *-h* have been shown to be the structural genes for the three Mg-chelatase subunits in barley (7, 8). The plant coding sequences homologous to *chlI* and *chlH* were cloned several years ago (9, 10). Recently, we identified a sequence homologous to the bacterial *bchD* gene and confirmed structural similarity between the bacterial and plant Mg-chelatase by expressing the CHL D, CHL I, and CHL H proteins from tobacco in yeast and measuring the activity of the recombinant enzyme complex in yeast extracts (11).

The enzymatic insertion of magnesium into protoporphyrin IX is catalyzed in two steps (12). First, an ATP-dependent activation complex is formed that consists of the subunits CHL D (Bch D) and CHL I (Bch I). When tested individually Bch I and Bch D had no ATPase activity, but when combined they hydrolyzed ATP (6, 13). In addition, the physical interaction between CHL D and CHL I as well as the homodimerization of CHL D were proven by the yeast two-hybrid system (11). In a second ATP hydrolyzing step, Mg^{2+} is inserted into protoporphyrin IX, which is most likely bound to CHL H (Bch H) (6).

The aim of this work was the elucidation of the enzymatic and interactive domains of CHL D. This subunit is known to be highly interesting because of its unusual structure (4, 11). The amino terminal half of CHL D shows significant similarity (46%) to the entire CHL I peptide sequence, indicating a duplication from an ancestral gene. The carboxyl-terminal moiety does not resemble any other known protein structure. Both parts of CHL D are linked by a glutamine/asparagine/proline-rich region, flanked by a highly acid-rich domain of more than 26 aa residues. In continuation of our previous work on the functional analysis of the Mg-chelatase subunits, we dissected CHL D and defined the essential regions for the interaction with the other subunits that were required for the enzymatic activity. For the functional investigations we assayed the recombinant subunits expressed in yeast. It is well known that enzymes of higher eukaryotic organisms are usually functional when expressed in yeast systems and that for this kind of study bacterial organisms are less suited (14). We established a functional model for the assembly of the interacting subunits needed for the active Mg-chelatase complex.

MATERIALS AND METHODS

Bacterial and Yeast Strains. *Eschericha coli* TG 1 [*supE* Δ (*hsdM-mrcB*) *5 thi* Δ(*lac-proAB*) F′ (*tra* Δ*36pro AB*$^+$ *lacI*^{q} *lacZ* Δ*M15*)] (New England Biolabs) hosted all plasmids. *E. coli* BL21 [F-*dcm ompT hsdS*(r_B-m_B-)*gal*] (Stratagene) was used for expression of the glutathione *S*-transferase (GST)-CHLD(M_1LM_2) fusion protein (Table 1, no. 3). All other GST fusion proteins were expressed in yeast strain CEN.PK2 (*MAT***a**/α, *ura*3–52/*ura*3/52, *trp*1–289/*trp*1–289, *leu*2–3/*leu*2–3, 112, *his*3–1/*his*3–1) (a kind gift of K.D. Entian, University of Frankfurt, Germany). Two-hybrid experiments and reconstitution assays of Mg-chelatase activity in yeast were performed in yeast strains SFY526 [*MAT***a**, *ura*3–52, *his*3–200, *ade*2–101, *lys*2–801, *trp*1–901, *leu*2–3, 112-*can*^{r}, *gal*4–542, *gal*80–538, *URA*3::*GAL*1$_{UAS}$-*GAL*1$_{TATA}$-

The publication costs of this article were defrayed in part by page charge payment. This article must therefore be hereby marked "*advertisement*" in accordance with 18 U.S.C. §1734 solely to indicate this fact.

PNAS is available online at www.pnas.org.

This paper was submitted directly (Track II) to the *Proceedings* office. Abbreviations: Chl, chlorophyll; Bch, bacteriochlorophyll; GST, glutathione *S*-transferase; N, N terminal; NM_1, N terminal and motif; NM_1LM_2, N terminal, motif, linker region, and motif; M_1LM_2, motif, linker region and motif; M_1LM_2C, motif, linker region, motif, and C terminal; M_2C, motif and C terminal; C, C terminal; AD, activating domain; BD, binding domain.

‡To whom reprint requests should be addressed. e-mail: fhaenel@pmail.hki-jena.de.

Table 1. The recombinant plasmid constructions used in this work

No.	Construct	Plasmid	CHL D fragment	Cloning sites
1	GST-CHL D(N)	pEGKT	63-374	*Bam*HI/*Hin*dIII
2	GST-CHL D(NM_1LM_2)	pEGKT	63-485	*Bam*HI/*Hin*dIII
3	GST-CHL D(M_1LM_2)	pGEX4T-1	375-485	*Bam*HI/*Eco*RI
4	GST-CHL D(M_1LM_2C)	pEGKT	375-748	*Xba*I/*Sal*I
5	CHL D	pGEM-7Zf(−)	63-748	*Xba*I/*Bam*HI
6	CHL I	pGEM-7Zf(−)	*ChlI*	*Xba*I/*Hin*dIII
7	CHL H	pCR II	*ChlH*	—
8	BD-CHL D(N)	pAS2-1	63-374	*Eco*RI/*Bam*HI
9	BD-CHL D(NM_1)	pAS2-1	63-398	*Eco*RI/*Bam*HI
10	AD-CHL D(NM_1)	pACT2	63-398	*Bam*HI/*Eco*RI
11	BD-CHL D(NM_1LM_2)	pAS2-1	63-485	*Eco*RI/*Bam*HI
12	AD-CHL D(NM_1LM_2)	pACT2	63-485	*Bam*HI/*Eco*RI
13	BD-CHL D(M_1LM_2)	pAS2-1	375-485	*Eco*RI/*Bam*HI
14	AD-CHL D(M_1LM_2)	pACT2	375-485	*Bam*HI/*Eco*RI
15	BD-CHL D(M_1LM_2)	pACT2-1	375-748	*Eco*RI/*Bam*HI
16	AD-CHL D(M_1LM_2C)	pACT2	375-748	*Bam*HI/*Eco*RI
17	BD-CHL D(M_2C)	pAS2-1	448-748	*Eco*RI/*Bam*HI
18	AD-CHL D(M_2C)	pACT2	448-748	*Bam*HI/*Eco*RI
19	BD-CHL D(C)	pAS2-1	486-748	*Eco*RI/*Bam*HI
20	(M_1LM_2C)CHL D-lexA	pFBL23	375-748	*Eco*RI/*Bam*HI
21	BD-CHL I-CHL D(M_1LM_2C)	pAS2-1	375-748	*Bam*HI/*Sal*I
22	CHL I	p423TEF	*ChlI*	*Sma*I/*Sal*I
23	AD-CHL D	pACT2	63-748	*Sma*I/*Eco*RI
24	AD-CHL I	pACT2	*ChlI*	*Sma*I/*Xho*I
25	AD-CHL H	pACT2	*ChlH*	*Sma*I/*Xho*I
26	BD-CHL D	pAS2	63-748	*Sma*I/*Sal*I
27	BD-CHL I	pAS2	*ChlI*	*Sma*I/*Sal*I
28	BD-CHL H	pAS2	*ChlH*	*Sma*I/*Sal*I

lacZ] (CLONTECH) and L40 [*MAT***a**, *his*3D200, *trp*1–901, *leu*2–3, 112, *ade*2, *LYS*2::($lexA_{op}$)$_4$-*HIS*3, *URA*3::($lexA_{op}$)$_8$-*lacZ*)] (a kind gift of S. Hollenberg, Fred Hutchinson Cancer Research Center, Seattle, WA).

Construction of Fusion Proteins Between CHL D Fragments and GAL4 Binding and/or Activation Domains or LexA-DNA Binding Domain. Plasmid isolation from *E. coli* was performed according to Sambrook *et al.* (15). Restriction enzymes Pwo-Polymerase and T4-Ligase were used as recommended by the manufacturers (GIBCO/BRL; AGS, Heidelberg). CHL D was dissected into N-terminal (N); N-terminal and motif (NM_1); N-terminal, motif, linker region and motif (NM_1LM_2); motif, linker region and motif (M_1LM_2); motif, linker region, motif and C-terminal (M_1LM_2C); motif and C-terminal (M_2C) and C-terminal (C) parts (Fig. 1). All fragments of *ChlD* were amplified by PCR using the plasmid pAS2-CHL D as template, sequenced, and cloned into two-hybrid plasmids pAS2–1, pACT2 (CLONTECH) and pFBL23 (14). N, NM_1, N M_1LM_2, M_1LM_2, M_1LM_2C, M_2C, and C (Table 1, nos. 8, 9, 11, 13, 15, 17, and 19) of *ChlD* were amplified by PCR, sequenced, and cloned into *Bam*HI/*Eco*RI-digested pAS2–1 by using the following synthetic oligonucleotides: 5′-GCT ATG GAT CCT AGC TTG GCT GCA GGT CGA CG-3′; 5′-AGA TAG GAT CCA ACT ATA GTT GAA CGT GGG AG-3′; 5′-AGA TAG GAT CCA CCT CTA TCT TCG GAA AAA GAT G-3′; 5′-AGA TAG GAT CCA AGC TTT CCA TCG ATG GCA GCT AAG CA-3′; 5′-AGA TAG GAT CCG AAT TCA TCT TTT CCG AAG ATA GAG GT-3′; 5′-AGA TAG AAT TCA TGG TGG AAC CTG AAA AAC AAC C-3′; 5′-AGA TAG AAT TCA TGG ATG CGG AAG GTG GTT TAG TG-3′; and 5′-AGA TAG AAT TCA TGT GCT TAG CTG CCA TCG ATG G-3′.

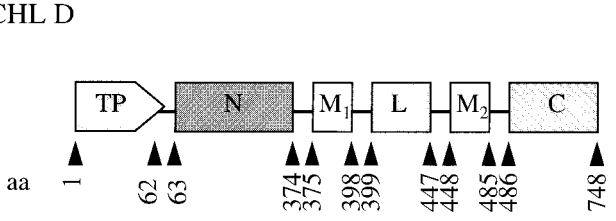

FIG. 1. The elements of the CHL D protein. TP, transit peptide; N, amino terminus; M_1 and M_2, peptide motifs 1 and 2; L, polyproline linker; C, the carboxy terminus. The amino acid positions (aa) are indicated below the elements.

The DNA fragments of NM_1, N M_1LM_2, M_1LM_2, M_1LM_2C, and M_2C of *ChlD* (Table 1, nos. 10, 12, 14, 16, and 18) were amplified by PCR, sequenced, and cloned into the *Eco*RI/*Bam*HI-digested pACT2 by using the following synthetic oligonucleotides: 5′-AGA TAG GAT CCA TGT GGA ACC TGA AAA ACA ACC-3′; 5′-AGA TAG GAT CCA TTG CTT AGC TGC CAT CGA TGG-3′; 5′-AGA TAG GAT CCG TGG AAC CTG AAA AAC AAC C-3′; 5′-AGA TAG AAT TCA ACT ATA GTT GAA CGT GGG AG-3′; 5′-AGA TAG GAT CCA TGA TGC GGA AGG TGG TTT AGT G-3′; 5′-AGA TAG AAT TCA CCT CTA TCT TCG GAA AAG ATG-3′; and 5′-AGA TAG AAT TCT AGC TTG GCT GCA GGT CGA CG-3′.

The DNA fragments of M_1LM_2C (Table 1, no. 20) of *ChlD* were amplified by PCR, sequenced, and cloned into *Eco*RI/*Bam*HI-digested pFBL23 (a kind gift of J. Camonis, Institut Curie, Paris) (16) by using the following synthetic oligonucleotides: 5′-AGA TAG AAT TCA TGT GCT TAG CTG CCA TCG ATG G-3′ and 5′-AGA TGG ATC CAG ATT CCT TGA ATG CAG ATA ATG C-3′.

Construction of the GST Fusion Proteins. The M_1LM_2 fragment of *ChlD* was amplified by PCR (primers: 5′-AGA TAG AAT TCA CCT CTA TCT TCG GAA AAG ATG-3′ and 5′-AGA TAG GAT CCT GCT TAG CTG CCA TCG ATG GA-3′), sequenced, and cloned into *Bam*HI/*Eco*RI-digested pGEX4T-1 (Table 1, no. 3; Amersham Pharmacia).

The N, N M_1LM_2, and M_1LM_2C fragments of *ChlD* were amplified by PCR (primers: 5′-GCT ATG TCG ACT AGC TTG

GCT GCA GGT CGA CG-3′; 5′-AGA TAG GAT CCG TGG AAC CTG AAA AAC AAC C-3′; 5′-AGA TAA AGC TTC TCT ATC TTC GGA AAA GAT G-3′; 5′-AGA TAG GAT CCA AGC TTT CCA TCG ATG GCA GCT AAG CA-3′, and 5′-AGA TCT CTA GAT TGC TTA GCT GCC ATC GAT GGA-3′), sequenced, and cloned into *Bam*HI/*Eco*RI (N-CHL D)-, *Bam*HI/*Hin*dIII (NM_1LM_2-CHL D), and *Xba*I/*Sal*I (M_1LM_2C-CHL D)-digested pEGKT (Table 1, nos. 1, 2, and 4) (12).

Cloning of *ChlI* and *ChlD* of Mg-Chelatase into the Cloning Vector pGEM7Zf(−). The vector pGEM-7Zf(−) (Promega) was used as a template for *in vitro* transcription experiments (Amersham Pharmacia; T7-transcription-translation kit) The DNA of *ChlI* and *ChlD* (Table 1, nos. 6 and 5) of Mg-chelatase of *Nicotiana tabacum* was amplified by PCR and sequenced. For the DNA amplification of *ChlI* the following primers were used: 5′-AGA TCT CTA GAT ATG GCT TCA CTA CTA GGA ACT TCC-3′ and 5′-GCT ATA AGC TTT AGC TTG GCT GCA GGT CGA CG-3′. *ChlI* was cloned into *Xba*I/*Hin*dIII-digested pGEM-7Zf(−). Primers for the DNA amplification of *ChlD* were: 5′-AGA TCT CTC GAT ATG GTG GAA CCT GAA AAA CAA CC-3′ and 5′-GCT ATG GAT CCT AGC TTG GCT GCA GGT CGA CG-3′. *ChlD* DNA was cloned into *Xba*I/*Bam*HI-digested pGEM-7Zf(−).

Two-Hybrid Analysis. Yeast transformation was performed according to Klebe *et al.* (17). *Saccharomyces cerevisiae* SFY526 (CLONTECH) was used as reporter strain. The β-galactosidase activity was assayed in a β-galactosidase filter-lift assay as described (18) and in liquid cultures (19). The filter assay is more sensitive than the liquid-culture assay and its results are more critical for quantification. The liquid-culture assay is less sensitive but better suited for quantification.

Mg-Chelatase Reconstitution Assay and HPLC Analysis of Porphyrins. The Mg-chelatase reconstitution assays in yeast were performed as described in Papenbrock *et al.* (11). For analysis of the porphyrin content, 200 μl of the assay mixture was extracted with 200 μl of methanol and centrifuged at 20,000 × *g* for 5 min. Porphyrins were analyzed in the methanol phase by HPLC with a Spherisorb S50D analytical column (4.6 × 250 mm) (Waters). The elution was performed by using a 25-min linear gradient from 5% (vol/vol) solvent A to 95% (vol/vol) solvent B at 1.5 ml/min. Solvent A contained 0.05% (vol/vol) triethylamine in water; solvent B contained 100% acetonitrile. Porphyrins were detected with a Shimadzu RF-551 fluorescence detector. Excitation was done at 420 nm and emission at 595 ± 5 nm to detect Mg protoporphyrin.

Purification of the GST Fusion Proteins in *E. coli* BL21 and *S. cerevisiae* CEN.PK2. Purification of the GST-CHL D(M_1LM_2) fusion protein (Table 1, no. 3) was performed as recommended by the manufacturer (Amersham Pharmacia). The GST-CHL D(N), (N M_1LM_2), and (M_1LM_2C) fusion proteins (Table 1, nos. 1, 2, and 4) were purified in yeast according to Mitchell *et al.* (14).

Affinity Chromatography of the GST Fusion Proteins *in Vitro*. Transcription/translation-experiments with CHL I, CHL D, and CHL H (Table 1, nos. 5–7) were carried out in reticulocyte lysate (T7-*in vitro* transcription/translation-system; Amersham Pharmacia) according to the manufacturer's protocol. The protein-binding assay was performed as described (20). Twenty micrograms of affinity-purified GST fusion protein was bound to 100 μl of glutathione-agarose (100 μg/ml) (Sigma) in the presence of 20 mM Hepes, pH 7.8/100 mM KCl/5 mM $MgCl_2$. A volume of 10 μl of the [^{35}S]methionine-labeled *in vitro*-translated protein was added and incubated for 90 min at 4°C to assay the specific interactions. The glutathione-agarose beads were washed four times in 20 mM Hepes, pH 7.8/100 mM KCl/5 mM $MgCl_2$/0.5 mM DTT/0.5% Igepal CA-630. The bound proteins were analyzed by SDS/PAGE and fluorography.

RESULTS

The Central CHL D Region of the Mg-Chelatase Mediates the Interaction Between CHL I and CHL D. Plant-specific cDNA sequences encoding all three Mg-chelatase subunits (Table 1) were characterized only in tobacco (1, 11, 21). The active Mg-chelatase could be expressed in yeast. The synthesis of the dissected recombinant CHL D protein in yeast allowed us to elucidate the protein–protein interactions between the various CHL D elements and the other subunits. The amino terminus of CHL D consisted of the transit peptide sequence responsible for the chloroplast targeting (amino acids 1–62; Fig. 1). In addition, it contained an amino acid sequence that was similar to CHL I (N, amino acids 63–374; Fig. 1), indicating its origin by an ancestral gene duplication. The carboxyl-terminal half (C, amino acids 486–748; Fig. 1) was linked to the amino terminus (N) by a glutamine/asparagine/proline-rich region (L, amino acids 399–477; Fig. 1), including a flanking area of 23 aa, 16 of which were negatively charged. In direct proximity to both sides of the linker molecule we identified a special protein motif (EK-X_{16}-R; M_1, amino acids 375–398 and M_2, amino acids 448–485; Fig. 1). An *in silico* analysis indicated that this sequence formed an amphipatic helix (22).

To perform the interaction analysis of the above CHL D fragments with the various subunits, we fused the truncated coding DNA segments of CHL D in-frame with the DNA-binding domain (BD; Fig. 2) of the yeast transcription factor GAL4 (*S. cerevisiae*/*E. coli* shuttle vectors pGBT9 and pAS2–1; Table 1, nos. 8, 11, 15, and 17). In addition, the DNA sequences encoding the CHL H, CHL I and CHL D proteins (Table 1, nos. 23–25) were fused in-frame with the transactivating domain (AD) of GAL 4 (pGAD424 and pACT2 vectors) and expressed in yeast.

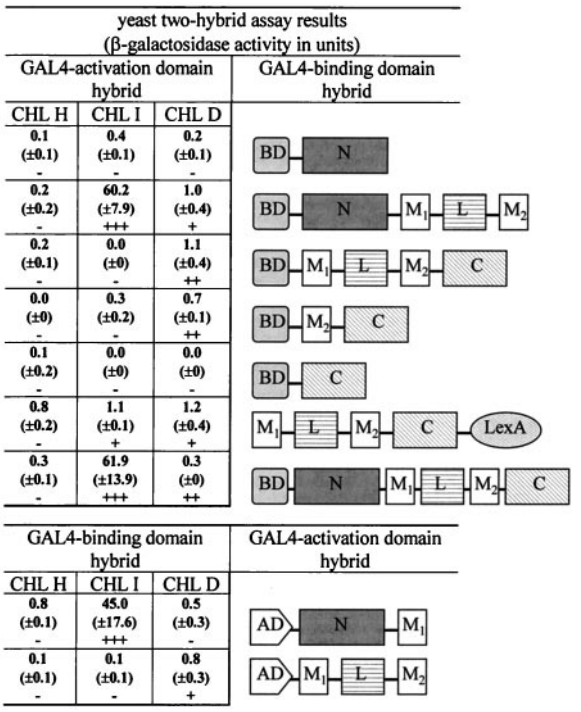

FIG. 2. Results of the interaction studies between the various constructs of CHL D with the CHL D, CHL I, or CHL H subunits of tobacco Mg-chelatase in the yeast two-hybrid system. (*Left*) The numbers indicate the β-galactosidase activity in units (mean value of three measurements) and in parentheses the corresponding SD. One unit is defined as the amount of protein required for the hydrolysis of 1 μmol of *o*-nitrophenol galactose per min and cell. + and − indicate the intensity of the indolyl compound of 5-bromo-4-chloro-3-indolyl β-D-galactoside (+++, strong; ++, intermediate; +, weak; −, no interaction). (*Right*) Gal4-activation (AD) and binding domains (BD). For abbreviations see Fig. 1,

The DNA of CHL D (M_1LM_2) was used exclusively in reciprocal fusion constructs [GAL4-AD-CHL D(M_1LM_2) + GAL4-BD-CHL I or GAL4-BD-CHL H or GAL4-BD-CHL D; Table 1, nos. 14 and 26–28] because in nonreciprocal constructs the β-galactosidase reporter gene was activated. The reason for this was the high acid-rich M_1LM_2 domain, closely related to the transactivating domains of various transcription factors (23). The reciprocal fusion construct between GAL4-AD-CHL D(NM_1) and CHL D (Table 1, nos. 10 and 26) also revealed greater β-galactosidase activities than the nonreciprocal fusion construct. The results of the two-hybrid assays are given either in β-galactosidase units as described by Munder and Fürst (ref. 19; Fig. 2) or were estimated according to the even more sensitive filter-lift assay by Breeden and Nasmyth (ref. 18; Fig. 2).

The amino terminal part of CHL D (amino acids 63–374; Table 1, no. 8) itself did not interact with any of the subunits of the Mg-chelatase. The segment M_1 fused to N (amino terminus CHL D) interacted with CHL I and very weakly with CHL H, but no homodimerization could be observed (Table 1, nos. 10 and 26–28). However, if CHL D(N M_1) was fused with both L and M_2, the interaction with CHL I and homodimerization was obtained (Table 1, nos. 14 and 27). An interaction between the carboxyl terminal part of CHL D (amino acids 486–748; Table 1, no. 19) and the subunits of the Mg-chelatase could not be observed. However, a fusion of the C-terminus CHL D fragment with M_2 and/or M_1LM_2 resulted in a dimerization only with CHL D (Table 1, nos. 15, 17, and 23). A lack of interaction between the C terminus together with M_1LM_2 [CHLD(M_1LM_2C)] and CHL I (Table 1, nos. 15 and 24) could be explained by a lacking accessibility of the central region to the interacting partner. To prove this assumption, a fusion protein of CHL D (M_1LM_2C) and the bacterial DNA-binding protein LexA at the C terminus (all GAL4-fusions were at the N terminus of the proteins) was tested against all three subunits in a yeast two-hybrid assay and showed an interaction with CHL I and a very weak interaction with CHL H (Table 1, nos. 20, 24, and 25). The linker region (amino acids 375–485; Fig. 1) of CHL D fused with GAL4-AD revealed only a weak interaction when coexpressed with GAL4-BD-CHL D (Table 1, nos. 14 and 26).

The Central Part of CHL D (Amino Acids 375–485) Also Interacts with CHL H. We also performed GST pull-down experiments to confirm both the homodimerization of CHL D and its interaction with CHL I. For this purpose nucleotide sequences encoding the amino acids 63–374 (N), 63–485 (N M_1LM_2), 375–485 (M_1LM_2), and 375–748 (M_1LM_2C) were fused to the gene encoding GST (Table 1, nos. 1–4). The GST-CHL D fusion proteins were expressed in *S. cerevisiae* and *E. coli* (GST-M_1LM_2), purified, and incubated with the radiolabeled, *in vitro*-produced CHL I, CHL D, or CHL H proteins (Table 1, nos. 5–7; Fig. 3). By this means, both GST-CHL D(N M_1LM_2) and GST-CHL D(M_1LM_2C) interacted with CHL I and CHL D (Table 1, nos. 2 and 4). The control experiments performed with only GST showed that the interaction between GST and CHL D as a control (Fig. 3*C*) was in a similar range compared with the GST-CHL D(NM_1LM_2) fusion protein. However, this finding was not surprising because this interaction was very weak (see two-hybrid experiments, Fig. 2). The other control experiments performed with only GST were negative (Fig. 3). These results coincided with the *in vivo* data found by using the two-hybrid system. However, no interaction could be found between GST-CHL D (N) (Table 1, no. 1) and the other proteins. In addition, the pull-down experiments revealed several interactions *in vitro* that could not be detected in the two-hybrid assays *in vivo*. The isolated M_1LM_2 fragment of CHL D interacted with CHL D and CHL I. Even more, with the exception of CHL D(N) (Table 1, no. 1), we could observe a weak interaction between all GST-CHL D fusion proteins and CHL H (Fig. 3).

The Protein Region M_1LM_2 Flanking the Polyproline Linker of CHL D and the Full-Length CHL I and CHL H Proteins Are Sufficient for Mg-Chelatase Enzyme Activity. The requirement

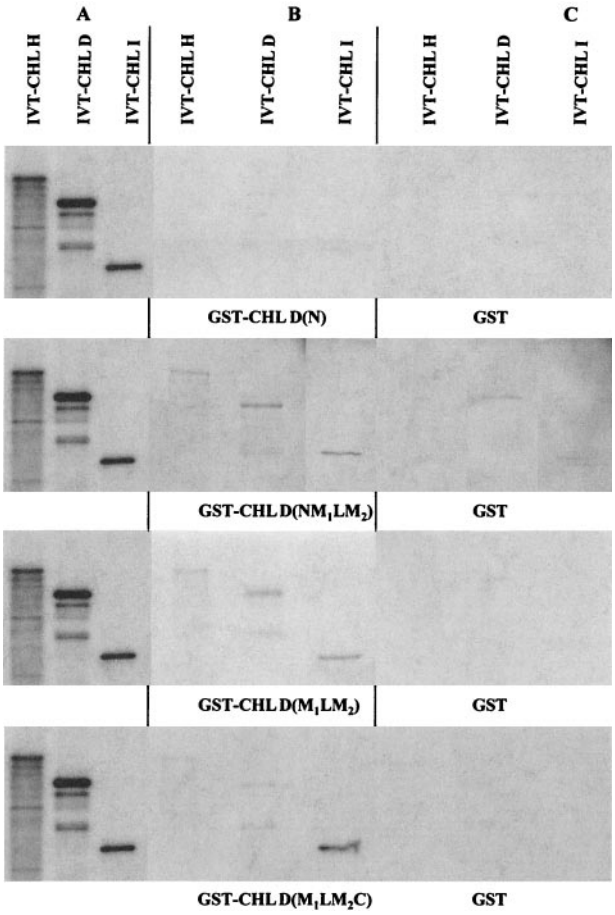

FIG. 3. *In vitro* interaction studies between the various peptide elements of CHL D and CHL D, CHL I and CHL H. (*A*) The *in vitro* translated (IVT) subunits of the Mg-chelatase CHL H, CHL D, and CHL I. On each track of the SDS/PAGE 20% of the protein subunits used for the interaction assays (*B* and *C*) were separated. (*B*) The results of interactions between the fusion proteins GST-CHLD(N), GST-CHLD(NM_1LM_2), GST-CHLD(M_1LM_2), GST-CHLD(M_1LM_2C) (see Table 1), and the *in vitro*-translated subunits CHL H, CHL D, and CHL I. (*C*) The interaction between GST and the *in vitro*-translated subunits CHL H, CHL D, and CHL I.

of Bch I/CHL I, Bch D/CHL D, and Bch H/CHL H was shown to be essential for Mg-chelatase activity in both bacteria and plants (3, 4, 11). Our fine-interaction analysis of the three tobacco subunits demonstrated that the central part of CHL D mediates the interaction between CHL D, CHL I, and CHL H. Therefore, truncated CHL D proteins were constructed to test whether the above interactions were sufficient to maintain the activity of the Mg-chelatase. First, the reporter strain SFY526 was cotransformed with the expression plasmids of CHL I and the GAL4 AD-CHL H fusion construct (Table 1, nos. 22 and 25). Subsequently, competent cells of this recombinant strain were transformed with different GAL4 BD-CHL D fusion constructs (Table 1, nos. 8, 9, 11, 13, 15, 17, and 19). Protein extracts of these yeast strains harboring the various combinations of expression plasmids were tested for Mg-chelatase activity (Fig. 4). Protein extracts containing CHL I, CHL H and CHL D(N), or CHL D(C) (Table 1, nos. 22, 25, 8, and 19, respectively) showed a slightly increased Mg-protoporphyrin IX concentration when compared with the background level. However, constructs of the amino and carboxyl-terminal parts of CHL D, fused with the M_1LM_2 motif, led to a 70- to 100-fold increase of Mg insertion into protoporphyrin IX. This activity corresponded to the maximum activity of the intact tobacco enzyme. Remarkably, the combination of the CHL D(NM_1) or CHL D(M_2C) fragment with CHL I and CHL H also resulted in a 40- to 70-fold increase of Mg-protoporphyrin

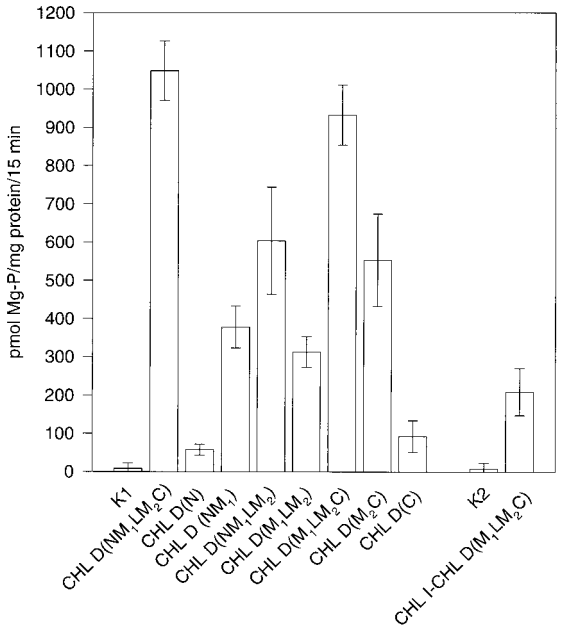

FIG. 4. Diagram of the Mg-chelatase activity of the CHL D constructs (see Table 1) in the presence of CHL I and CHL H. The activity is given in pmol Mg-protoporphyrin IX (Mg-P)/mg protein per 15 min. The SDs were calculated from three independent experiments. K1 and K2 indicate the controls showing the Mg-chelatase activity from yeast cells expressing CHL I and CHL H and solely expressing the artificial I-D fusion protein, respectively.

IX formation (Table 1, nos. 10, 18, 22, and 25). In addition, we expressed the M_1LM_2 region of CHL D in combination with CHL H and CHL I in *S. cerevisiae* (Table 1, nos. 13, 25, and 22, respectively), which resulted in a 40-fold accumulation of protoporphyrin IX in relation to the background (Fig. 4).

In conclusion, CHL D(N) or CHL D(C) were not sufficient to achieve Mg-chelatase activity, indicating that the central M_1LM_2 region was essential for the activation of the protoporphyrin IX chelation reaction. Moreover, one of the two M domains was already sufficient for Mg-chelatase catalysis (40-fold increase; Fig. 4).

In an additional approach to further minimize the Mg-chelatase complex, the amino terminal half of CHL D (CHL D(N) was substituted by CHL I (Table 1, no. 21). The fusion gene encoding CHL I-CHL D(M_1LM_2C) was coexpressed with a gene for CHL H in yeast, and the peptide extract was assayed for Mg-chelatase activity. As shown in Fig. 4, the protein extract that contained only two recombinant peptides yielded a Mg-chelatase activity of 209 pmol Mg-protoporhyrin IX/mg of protein per 15 min. This result corresponded to a 20-fold increase of Mg-protoporphyrin IX accumulation.

DISCUSSION

Three proteins (CHL I, CHL D, and CHL H) (11) are implicated to obtain an active Mg-chelatase complex in all bacterial and plant sources studied so far. CHL D has the most interesting and complex protein structure. It is composed of three different domains (see Fig. 1). The magnesium-insertion step of chlorophyll biosynthesis is a two-stage reaction (3, 6, 12). For the first step, i.e., the preactivation of the Mg-chelatase, both bacterial proteins Bch I and Bch D (corresponding to CHL I and CHL D in plants) in the presence of ATP and magnesium are required (3, 6). Recently, we demonstrated a direct interaction between CHL I and CHL D coinciding with the preactivation step (11). In the present work an extended analysis was performed to localize the precise interaction sites of the CHL D domain and to determine their function. Our data proved that the protein domains M_1 and M_2, flanking the polyproline linker L of CHL D, fulfill the structural demands for a homodimerization and the interaction between CHL I and CHL D, respectively (Fig. 2). Both M_1 and M_2 contain the common peptide sequence EK-X_{16}-R (Fig. 1) and were shown *in silico* (software: HELICALWHEEL, HUSAR, Heidelberg) to form a potential amphipathic helix (Fig. 5). Similar results were obtained for the corresponding sequences in *Pisum sativum* and *Synechocystis* (data not shown). Our functional dissection of the CHL D protein revealed that only M_1LM_2, i.e., the proline-rich region plus the two flanking EK-X_{16}-R motifs (Fig. 1), were required for the basic activity of the Mg-chelatase, provided that they interacted with both CHL I and CHL H (Fig. 3). The Mg-chelatase was shown to have a reduced activity upon removal of the amino-terminal and the carboxyl-terminal parts of CHL D. This reduction could be partially explained by the missing ATPase binding element situated at the N terminus. However, when these termini were compared in respect to their contribution to the enzyme activity, the C terminus was much more important than the N terminus (Fig. 4). This result was quite surprising because the C terminus did not show any similarity to other known important protein elements. An additional aspect of interest was the high similarity (46%) between the N terminus of CHL D and the CHL I protein. Therefore, we investigated the question of whether the N terminus of CHL D could be replaced by CHL I without any loss of enzyme activity. A fusion protein between CHL I and CHL D(M_1LM_2C) (Table 1, no. 21) was coexpressed with the CHL H protein in *S. cerevisiae*. Surprisingly, this revealed an activity of only approximately 20% (Fig. 4) when compared with the native enzyme, indicating that the N terminus of CHL D was functionally different from CHL I, despite their high sequence homology.

Considering our own data, the model of the Mg-chelatase action presented by Walker and Willows (1) could be improved. They proposed that during preactivation one D subunit dissociates from a (4D)-aggregate and associates with four I dimers to form a ($4I_2$)-D complex. The complex formation is ATP dependent, and the model shows phosphorylation by a protein kinase in this step. For the chelation step, the ($4I_2$)-D complex associates

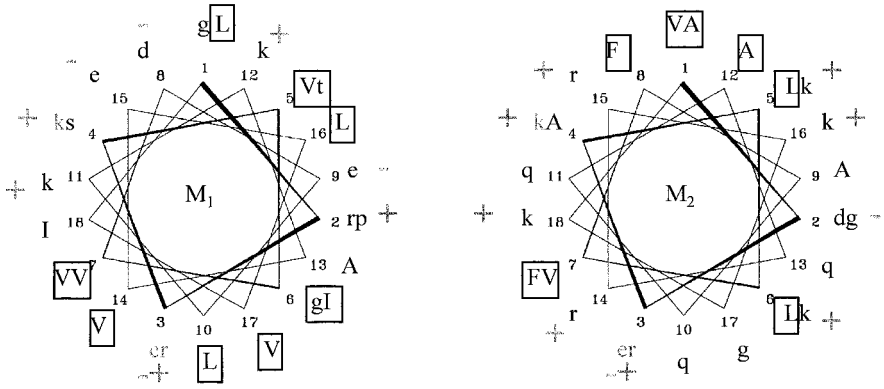

FIG. 5. Helical wheel plots of the protein motifs M_1 and M_2 of CHL D (see also Fig. 1). Hydrophobic amino acids are indicated by filled boxes. Charged amino acids are indicated by + and −. The numbers indicate the positions of the corresponding amino acids in the helix.

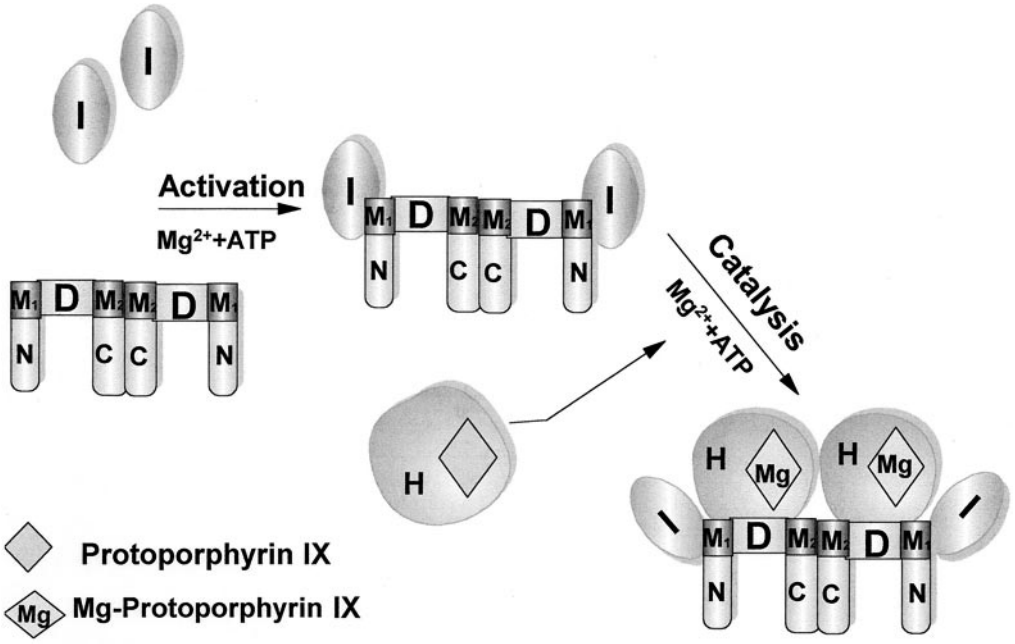

FIG. 6. Model of the mechanism of the Mg-chelatase (stoichiometry not regarded). The protein D units occur initially at least as dimers (eventually as multimers) and I as a monomer. In the preactivation step, which is magnesium and ATP dependent, the I proteins interact with the M_1 motifs of the CHL D subunits. The CHL D subunits are dimerized or multimerized involving the M_2C domains of D. In the chelation step, the H protein subunits interact with the M_1LM_2 region of CHL D.

with four H subunits and the (4H)-($4I_2$)-D complex catalyzes the insertion of magnesium into protoporphyrin IX. The insertion of magnesium is also ATP dependent. The model suggests that the I and H subunits participate in catalysis and the D subunit only in preactivation. This prediction is based solely on stoichiometry rather than properties of the subunits.

We assigned a central role in the enzymatic complex to CHL D. Our data showed that protein D is capable of forming at least dimers, i.e., eventually even multimers. In addition, we proved that protein D interacted with both CHL I and CHL H. The minimum requirement for these interactions was the M_1LM_2 element of protein D. Furthermore, in previous work (11), we were able to show that no homodimerization of CHL I and no protein–protein interaction between CHL I and CHL H occurred. Therefore, in our model (Fig. 6) we show a preactivation complex composed of one D dimer and two I monomers. However, this proposal does not implicate the precise stoichiometry of the partners forming this complex. As described (13), the D/I-complex showed ATPase activity. The hydrolysis of ATP might be crucial for the preactivation step, providing the system with energy. In contrast to the previous model, we showed that phosphorylation of the subunit D cannot play a role for the preactivation step. This demonstration was done by expressing the minimum M_1LM_2 element, containing one eukaryotic phosphorylation site, in *E. coli*. Using this method we still saw interaction between M_1LM_2 and CHL I (Fig. 3).

In the chelation step (Fig. 6), it was suggested by Petersen and colleagues (5) that the CHL H-protoporphyrin IX complex interacts transiently with the ternary complex CHL I/CHL D/ATP/Mg^{2+}. It remains open whether or not the CHL I subunit is still needed for the chelation step (Fig. 6). We suppose that CHL D plays a central role in the final complex responsible for the transfer of Mg^{2+} to protoporphyrin IX, which was shown to be attached to CHL H (6, 24). The hypothesis that CHL D might bind Mg^{2+} also is suggested in a recent publication by Jensen and colleagues (25).

In summary, our model (Fig. 6) involves, in analogy with the former one (1), both a preactivation and a chelation step. However, initially the protein D subunits occur as dimers and/or multimers, and the subunit I as a monomer. In the preactivation step, which is magnesium and ATP dependent, the I proteins interact with the NM_1 domain of the CHL D subunits. Furthermore, the CHL D subunits are dimerized or multimerized involving the M_2C domains of D. In the following chelation step, the H protein subunits interact with the M_1LM_2-region of CHL D. Thereby, it still remains unclear whether for the second step, i.e., the chelation process, all three subunits were needed. Although many steps of our model could be experimentally supported, several aspects, such as the stoichiometry, remain open and have to be further investigated.

We are indebted to K. D. Entian, S. Hollenberg, and J. Camonis for yeast strains and plasmids. In addition, we thank H. Krügel for critically discussing the manuscript. The work was supported by Bundesministerium für Bildung, Wissenschaft, Forschung und Technologie Grant 0311073A.

1. Walker, C. J. & Willows, R. D. (1997) *Biochem. J.* **327,** 321–333.
2. Al-Karadaghi, S., Hansson, M., Nikonov, S., Jönsson, B. & Hederstedt, L. (1997) *Structure (London)* **5,** 1501–1510.
3. Gibson, L. C. D., Willows, R. D., Kannangara, C. D., von Wettstein, D. & Hunter, C. N. (1995) *Proc. Natl. Acad. Sci. USA* **92,** 1941–1944.
4. Jensen, P. E., Gibson, L. C. D., Henningsen, K. W. & Hunter, C. N. (1996) *J. Biol. Chem.* **271,** 16662–16667.
5. Petersen, B. L., Jensen, P. E., Gibson, L. C. D., Stummann, B. M., Hunter, C. N. & Henningsen, K. W. (1998) *J. Bacteriol.* **180,** 699–704.
6. Willows, R. D., Gibson, C. D., Kanangara, C. G., Hunter, C. N. & von Wettstein, D. (1996) *Eur. J. Biochem.* **235,** 438–443.
7. Jensen, P. E., Willows, R. D., Petersen, B. L., Vothknecht, U. C., Stummann, B. M., Kannangara, C. G., von Wettstein, D. & Henningsen, K. W. (1996) *Mol. Gen. Genet.* **250,** 383–394.
8. Kannangara, C. G., Vothknecht, U. C., Hansson, M. & von Wettstein, D. (1997) *Mol. Gen. Genet.* **254,** 85–92.
9. Koncz, C., Meyerhofer, R., Koncz-Kalman, Z., Nawrath, C., Reiss, B., Redei, G. P. & Schell, J. (1990) *EMBO J.* **9,** 1337–1346.
10. Hudson, A., Carpenter, R., Doyle, S. & Coen, E. S. (1993) *EMBO J.* **12,** 3711–3719.
11. Papenbrock, J., Gräfe, S., Kruse, E., Hänel, F. & Grimm, B. (1997) *Plant J.* **12,** 981–990.
12. Walker, C. J. & Weinstein, J. D. (1994) *Biochem. J.* **299,** 277–284.
13. Hansson, M. & Kannangara, G. (1997) *Proc. Natl. Acad. Sci. USA* **94,** 13351–13356.
14. Mitchell, D. A., Marshall, T. K. & Deschenes, R. J. (1993) *Yeast* **9,** 715–723.
15. Sambrook, J., Fritsch, E. F. & Maniatis, T. (1989) *Molecular Cloning: A Laboratory Manual* (Cold Spring Harbor Lab. Press, Plainview, NY), 2nd Ed.
16. Beranger, F., Aresta, S., de Gunzburg, J. & Camonis, J. (1997) *Nucleic Acids Res.* **25,** 2035–2036.
17. Klebe, J. K., Harris, J. V., Sharp, D. & Douglas, M. G. (1983) *Gene* **25,** 333–341.
18. Breeden, L. & Nasmyth, K. (1985) *Cold Spring Harbor Symp. Quant. Biol.* **50,** 643–650.
19. Munder, T. & Fürst, P. (1992) *Mol. Cell. Biol.* **12,** 2091–2099.
20. Peukert, K., Staller, P., Schneider, A., Carmichael, G., Hänel, F. & Eilers, M. (1997) *EMBO J.* **16,** 5672–5686.
21. Kruse, E., Mock, H. P. & Grimm, B. (1997) *Plant Mol. Biol.* **35,** 1053–1056.
22. Tripet, B., Yu, L., Bautista, D. L., Wong, W. Y., Irvin, R. T. & Hodges, R. S. (1996) *Protein Eng.* **9,** 1029–1042.
23. Blau, J., Xiao, H., McCracken, S., O'Hare, P., Greenblatt, J. & Bentley, D. (1996) *Mol. Cell. Biol.* **16,** 2044–2055.
24. Hinchigeri, S. B., Hundle, B. & Richards, W. R. (1998) *FEBS Lett.* **407,** 337–342.
25. Jensen, P. E., Gibson, L. C. D. & Hunter, C. N. (1998) *Biochem. J.* **334,** 335–344.